



Open Archive Toulouse Archive Ouverte (OATAO)

OATAO is an open access repository that collects the work of Toulouse researchers and makes it freely available over the web where possible.

This is an author-deposited version published in: <http://oatao.univ-toulouse.fr/>
Eprints ID: 8685

To link to this article : DOI:10.4028/www.scientific.net/MSF.654-656.890
URL: <http://dx.doi.org/10.4028/www.scientific.net/MSF.654-656.890>

To cite this version:

Huez, Julitte and Buirette, Christophe and Andrieu, Eric and Pérusin, Simon and Audion, Sylvain *Characterization of the Mechanical Behaviour of Both Fusion Zone and Base Metal of Electron Beam Welded TA6V Titanium Alloy*. (2010) *Materials Science Forum*, vol. 654-656. pp. 890-893. ISSN 0255-5476

Any correspondence concerning this service should be sent to the repository administrator: staff-oatao@listes.diff.inp-toulouse.fr

Characterization of the mechanical behaviour of both fusion zone and base metal of electron beam welded TA6V titanium alloy.

HUEZ Julitte^{1,a}, BUIRETTE Christophe^{1,b}, ANDRIEU Eric^{1,c}, PERUSIN Simon^{2,d} and AUDION Sylvain^{2,e}

¹Université de Toulouse, Institut Carnot CIRIMAT, ENSIACET, 4 allée Emile Monso 31432 Toulouse- France

²Airbus Operations SAS, 316 Route de Bayonne, 31060 Toulouse cedex 9- France

^ajulitte.huez@ensiacet.fr, ^bchristophe.buirette@ensiacet.fr, ^ceric.andrieu@ensiacet.fr, ^dsimon.perusin@airbus.com, ^esylvain.audion@airbus.com

Keywords: Titanium alloy, Ti-6Al-4V, electron beam welding, heat treatment, impact toughness.

Abstract. The fusion zone of an electron beam welded Ti-6Al-4V alloy presents a α' martensitic structure which leads to a change of mechanical properties. Starting from two manufacturing processing routes for the alloy (1) a β processing followed by the weld (which will be considered as the reference microstructures), (2) an $\alpha+\beta$ processing followed by welding and a post weld heat treatment (PWHT), the microstructure can be adjusted to avoid local difference of strength, fatigue properties and impact toughness. This results from the optimisation of the process and of the PWHT. The present work investigates the mechanical behaviour and the damage mechanism of both base metal and fusion zone in regards to the microstructure and to the heat treatment parameters.

Introduction

Electron beam welding offers new assembling solutions for the development of aeronautics structure parts. One of its inherent challenge is to enhance the mechanical properties of the weld. Previous results [1-2] pointed out that a supertransus PWHT on the welded $\alpha+\beta$ Ti-6Al-4V alloy allows to homogenise the entire microstructure, and then to enhance the impact toughness simultaneously in the fusion zone and the base metal. Impact toughness and tensile tests have been conducted to explore the dynamic and static behaviour of the different microstructures found in these welded plates, and to describe the fracture path. Progress in understanding of damage mechanisms requires a particular attention to the specimen's orientation and crack propagation in relation to the possible anisotropy of the alloy.

Experimental procedure

Two rolled plates of Ti-6Al-4V alloy (12 mm thick), respectively β and $\alpha+\beta$ annealed, were used. They will be denoted (β) and ($\alpha+\beta$). The chemical composition of the plate is given in Table 1.

Table 1 : Chemical composition [% wt] of the Ti-6Al-4V alloy.

Element	Al	V	Fe	C	N ₂	O ₂	H ₂	Ti
[%wt]	6.41	3.93	0.16	0.004	0.008	0.18	0.0039	matrix

Electron beam welding is carried out on each plate with a beam voltage of 65kV, a beam current of 170mA and a welding speed of 1m/min. Then, a stress relieving heat treatment of 5h at 650°C is carried out. The base metals and the welds microstructures are shown in Fig.1a & d. The base metal (BM) of the β and of the $\alpha+\beta$ annealed alloys consist respectively in a Widmanstätten α with a prior β grains and in a fine equiaxed α of an average grain size of 20 μm microstructures (Fig.1b & e). Both fusion zones (FZ) are constituted of α' martensite in prior β grains (Fig.1c). These last are elongated, with a length of 1mm for a width of 300 μm in the ($\alpha+\beta$)FZ while they are bigger and more compact in the (β) FZ with a length of 1,5 mm and a width of 1mm. This could be explained

by the heredity of the initial microstructure. A heat affected zone (HAZ) is also visible, but only in the $(\alpha+\beta)$ weld and it is noticed that even micro hardness measures carried out on a cross section of (β) weld plate do not reveal HAZ (Fig.1a and Table 2).

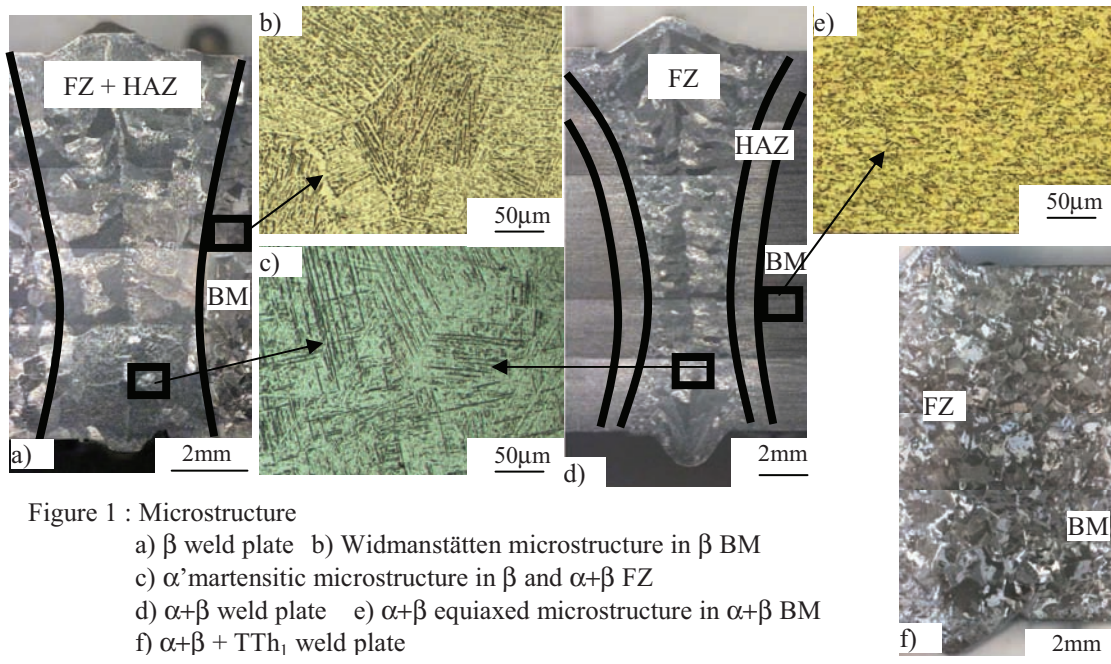


Figure 1 : Microstructure

- a) β weld plate
- b) Widmanstätten microstructure in β BM
- c) α' martensitic microstructure in β and $\alpha+\beta$ FZ
- d) $\alpha+\beta$ weld plate
- e) $\alpha+\beta$ equiaxed microstructure in $\alpha+\beta$ BM
- f) $\alpha+\beta + TTh_1$ weld plate

Table 2 : Microhardness values obtained with a mass of 200mg on different microstructures of Ti-6Al-4V alloy.

Microhardness	β MB	β ZF	$\alpha+\beta$ MB	$\alpha+\beta$ ZF	$\alpha+\beta$ HAZ
HV 0,2	330+/-40	370+/-10	310+/-10	370+/-10	350+/-20

Two supertransus PWHT, denoted TTh_1 and TTh_2 , have been achieved on $(\alpha+\beta)$ samples of approximately 800 mm^3 , differing essentially by the soaking time spent above the β transus : 48 min at 1030°C for TTh_1 against 10 min for TTh_2 . Fig.1f shows the microstructure resulting from the TTh_1 . i.e. an homogeneous Widmanstätten microstructure in the entire plate with a prior β grain size of $500 \mu\text{m}$. Similar microstructure is obtained after TTh_2 , but with a prior β grain size of $200 \mu\text{m}$. Fig.2a summaries the type, the orientation and the localization of the tested specimens. In a Rolling direction/Width/Thickness plate referential, the first letter of a specimen indicates the plane to which the notch is normal to, and the second letter indicates the direction of crack propagation. Samples will be referenced as followed : material (β , $\alpha+\beta$, $\alpha+\beta + TTh_1$, $\alpha+\beta + TTh_2$) / localization (MB, ZF) / orientation (WT, WR, RT, RW). Fig.2b & c presents the geometry of each specimen. The choice of non standard Charpy specimens has been previously discussed [1].

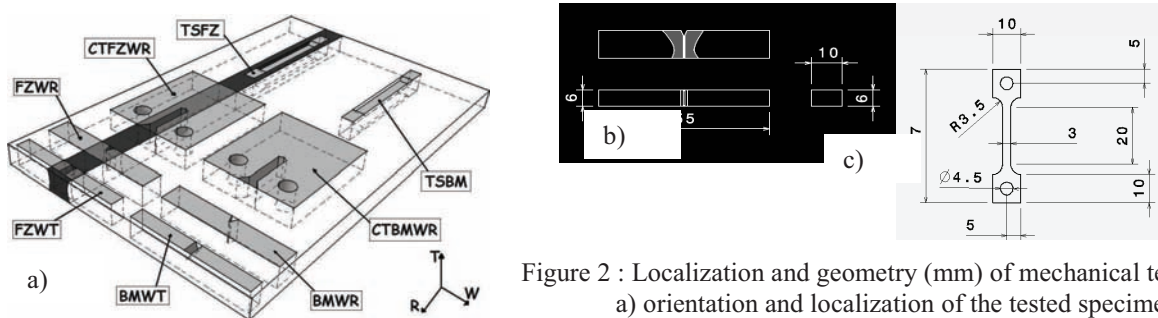


Figure 2 : Localization and geometry (mm) of mechanical test specimens
a) orientation and localization of the tested specimens
b) geometry of non standard Charpy specimens
c) geometry of tensile specimen
CT specimens are CT 75W B10

Results and discussion

First of all, the results comparing the FZ and BM of both processing routes (leading to (β) or to $(\alpha+\beta)$) will be discussed. For both plates, the α' martensitic microstructure present in the FZ

explains why the tensile specimens machined in this zone exhibit significantly higher strength level than the BM ones, whereas their ductility is quite low (Fig. 3a) [3]. $(\alpha+\beta)$ BM presents a high ductility correlated to the well known equiaxed α microstructure resistance nucleation of voids. These results fit with the value of microhardness presented in Table 2.

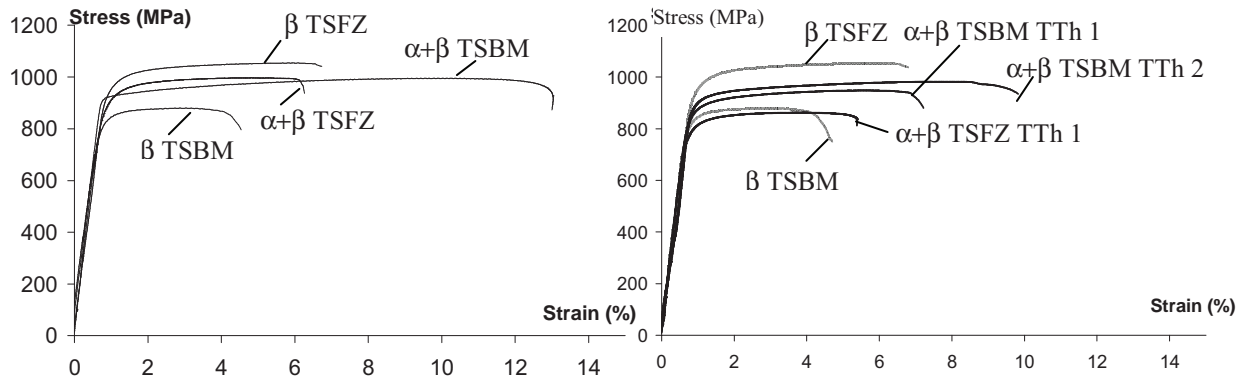


Figure 3 : a) tensile curves for (β) and $(\alpha+\beta)$ weld plates b) effect of PWHT on tensile tests

(β) BM demonstrates the lowest tensile properties whereas (β) BMWT presents the highest absorbed impact energy of 21,7 J (Fig. 4), which is confirmed by the fracture surface observation. Indeed, Fig. 6e points out that the β BMWT has the most tortuous appearance with a long fracture path profile when compared to (β) FZWT, $(\alpha+\beta)$ BMWT and $(\alpha+\beta)$ FZWT. This could be explained by the presence of the Widmanstätten microstructure where the thick α platelets and the prior β grain boundaries are deviating the fracture path [4]. These two microstructural parameters are also among those implied in the difference of propagation velocity between (β) FZ and (β) BM as observed on experimental kinetic crack growth diagrams $da/dN = f(\Delta K)$, especially in the low stress intensity range (Fig. 5). These tests on CTW75B10 specimens underline that the propagation rate in (β) CTFZWR is almost twice of the one in (β) CTBMWR.

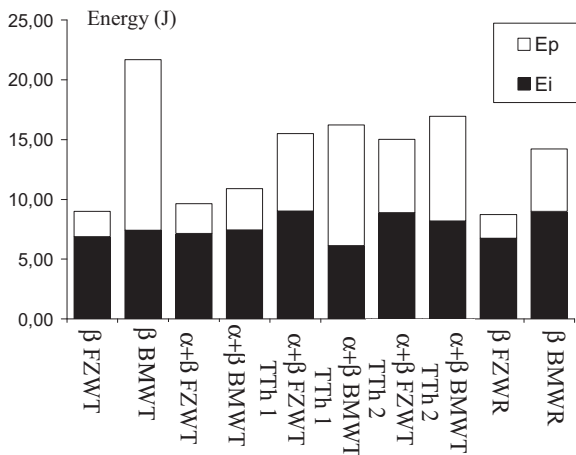


Figure 4 : Results of Charpy impact tests. The total absorbed energy $E_t = E_i$ (the apparent crack initiation energy) + E_p (the apparent crack propagation energy).

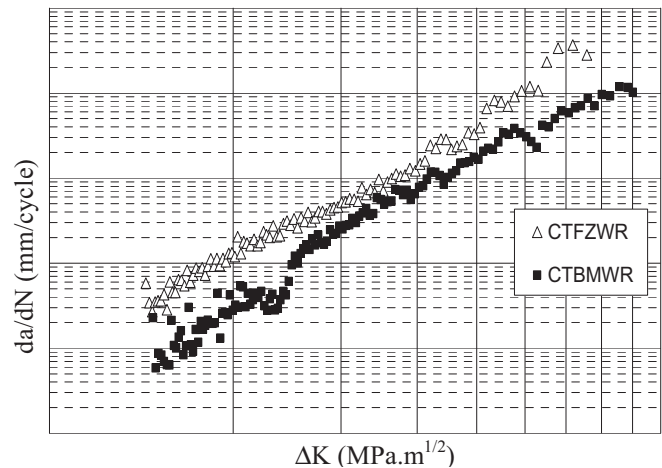


Figure 5 :Kinetic crack growth diagrams $da/dN=f(\Delta K)$ on (β) CTFZWR and (β) CTBMWR specimens

In this specimen as in all specimens where the notch is weld centred, it is noticeable that the crack follows the weld solidification front underlined by the α_{GB} grain boundary phase. Shifting slightly the notch from the weld centre could allow to describe the behaviour of the material in less favourable propagation conditions. To complete these results and observations, two others impact tests were performed on (β) FZWR and (β) BMWR, to obtain the propagation of the fracture in the same plane and same direction than for kinetic crack growth tests. Both weld centred impact tests, (β) FZWT and (β) FZWR, present the same low absorbed energy E_t of around 9 J. and the same

smooth fracture surface, probably due again to a preferential α_{GB} crack path. However, (β)BMWT and (β)BMWR specimens which give a E_t respectively of 21,7 J and of 14,2 J reveal anisotropic damage behaviour through their fracture surface as it is evidenced on Fig 6e & j : (β)BMWT has a ductile intergranular fracture mode whereas (β)BMWR presents cleavage features. This could be due to an anisotropy of the material and/or to a microstructural heterogeneity in the plate thickness. Crystallographic texture analysis of the (β) plate will help to clarify this result.

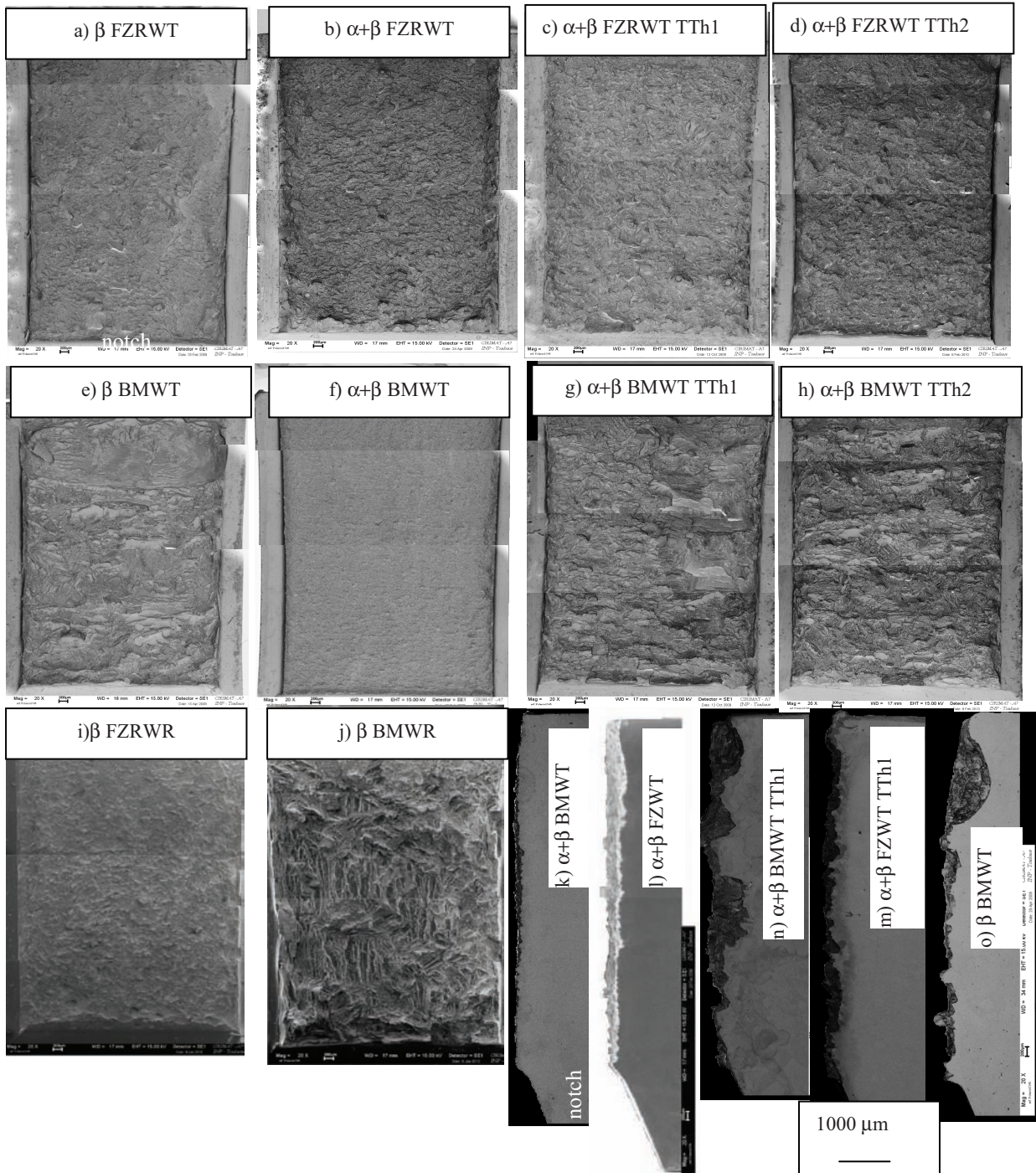


Figure 6 : Fracture surfaces and crack paths view in a median cross section perpendicular to the fracture surface of impact toughness specimens.

Secondly, we focus on the influence of the supertransus PWHT on mechanical responses of (α + β) weld plate, correlated to the homogenised Widmanstätten microstructure issue from this treatment. In terms of impact toughness in WT orientation, both PWHT gives a quite elevated absorbed energy of around 15 J. One more time, as it is visible on Fig. 6c, d, g, h, n & m, this energy is associated to a more irregular and rougher fracture surface and crack profile. In the FZ it is noticeable that the

solidification front, distinguished as a preferential fracture way, has disappeared. The fracture mode still mainly ductile but presents also some faceted intergranular appearance associated to a α_{GB} . This E_t is lower than the one obtained on the reference material (β)MBWT but higher than in the (β)FZWT. Another interest of the supertransus PWHT is its propensity to improve the tensile properties (Fig. 3b). The ductility obtained on ($\alpha+\beta$)TSBM TTh₁ and ($\alpha+\beta$)TSBM TTh₂ is enhanced as is, to a lesser extent, the one of ($\alpha+\beta$)TSFZ TTh₁. Other tests, as the one on ($\alpha+\beta$)TSBM TTh₂ which lets believe that its smallest prior β grains size will benefit to the ductility, but also other PWHT conditions, are on the route. Indeed, these first results are very encouraging for finding, with the control of the microstructure, the optimized supertransus PWHT in order to reach the best compromise between static and dynamic mechanical properties on the ($\alpha+\beta$) welded plate.

Conclusions

A solution to avoid microstructure heterogeneity due to the weld operation on β annealed Ti-6Al-4V, and its corresponding variation in mechanical properties, seems to be to start from a $\alpha + \beta$ annealed state and then to realized a supertransus PWHT. The soaking time spent above the transus is one of the most important parameters to adjust the final microstructure in terms of prior β grains size and α platelets thickness, together with the cooling rate and the initial equiaxed microstructure of the plate. Instrumented impact toughness tests are of first interest to improve the PWHT and to understand the associated damage mechanisms. They also point out the anisotropy of the material.

References

- [1] C. Buirette, J. Huez, S. Perusin and S. Audion : In TMS Annual Meeting, Seattle, (2010).
- [2] T. Mohandas, D. Banerjee, V. V. Kutumba Rao, Materials Science and Engineering A, 254 (1998), p. 147
- [3] G. Lütjering, J.C. Williams, Titanium, 2003, Springer, ISBN 3-540-42990-5.